W24: Investigating electronic structure with a single-axis tunneling microscope

Joshua P. Veazey,[1] Randy Lindgren,[1] Tikran Kocharian,[2] and Karl Brakora[2]

[1]*Physics Department, Grand Valley State University, 117 Padnos Hall of Science, 1 Campus Drive, Allendale, MI 49401*
[2]*School of Engineering, Grand Valley State University, 136 Kennedy Hall, 301 West Fulton St., Grand Rapids, MI 49504*

We have developed a simplified alternative to the scanning tunneling microscope (STM) that restricts tip motion to one dimension: the z-axis tunneling microscope (ZTM). Here, the z-axis lies along the tip-sample separation. Students are able to observe the exponential dependence on tunneling current with tip-sample gap and observe qualitative differences in the electronic density of states between metals, semimetals, and semiconductors. The current pre-amp and signals for the stepper motor, piezo actuator, and bias voltage are integrated into a single PC board. A second pc board routes signals to the DAQ and houses a power supply that connects to line voltage. All signals are either analog <10 V or TTL, allowing either manual or programmatic control. The ZTM is simpler and less costly to build than an STM, expanding access to a subset of STM experiments to more learners.

I. INTRODUCTION

The AAPT Recommendations for the Undergraduate Physics Laboratory Curriculum [1] provide a useful framework for designing advanced lab experiences for undergraduates. Solid state physics experiments in particular can expose students to technical and practical skills, as called for in the AAPT recommendations. A triumph of solid state physics has been in understanding macroscopic electronic properties of solids through their band structure. There is even richer physics to be found when investigating electronic properties using microscopic and nanoscale methods.

One way to probe local, energy-resolved electronic structure of solids is through vacuum tunneling into a sharp metallic tip [2]. The differential tunneling conductance dI/dV is proportional to the electronic density of states and can reveal information about band structure and surface states [3]. While vacuum may improve precision, for many materials it is not required. These include highly-oriented pyrolytic graphite (HOPG), which has been studied in ambient air [4] and water [5]. In addition to density of states, tunneling current as a function of tip-sample separation can be used to observe the exponential dependence of the tunneling probability on barrier width, extracting the work function in the process [2].

Traditionally, these sets of experiments are carried out using a scanning tunneling microscope (STM), where the metallic tip is raster-scanned laterally across the surface. The exponential dependence of the tunneling probability on the tip-sample spacing leads to very high spatial resolution, resolving atomic lattices in real space for many materials. The STM tip is stopped in place to perform tunneling spectroscopy (dI/dV vs. V) or current vs. tip-sample spacing (I-z). However, at many 4-year college and university institutions, STM may not exist, and even education-grade STM may be cost-prohibitive.

Previously, we reported the development of a simpler device, the z-axis tunneling microscope (ZTM) [6]. Figure 1 shows a simple schematic of the experimental system. Tip motion is limited to the z-axis (tip-sample spacing) by a 1D piezo transducer. The device is capable of tunneling spectroscopy via I-V and I-z. We piloted the device in a junior-level advanced laboratory course. Since that time, we continued work that we will discuss in this paper. We further developed the curricular materials for students with little or no background in electronic structure. We also integrated the electronic controls to make the ZTM into a more standalone instrument. PC board drawings and plans have been made

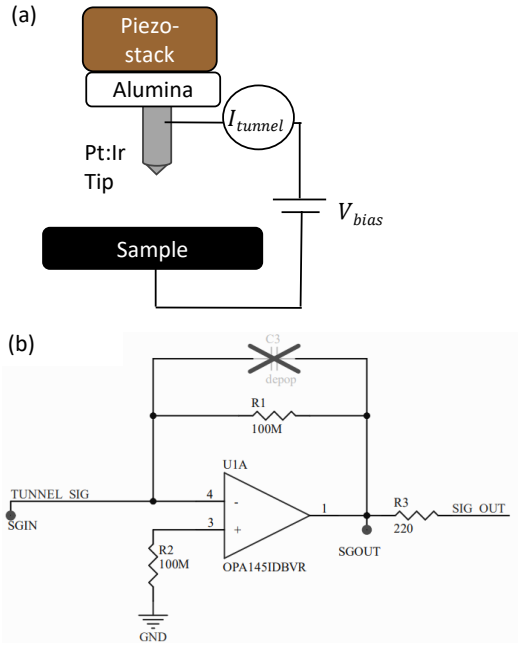

FIG. 1. (a) Simplified schematic of the scan head. A piezo stack (Thorlabs PC4FL) acts as a 1D actuator to adjust tip-sample spacing (tunneling barrier width). The V_{bias} is applied to the sample, relative to the same reference as the op-amp in the current-voltage pre-amp circuit (b). The pre-amp circuit is composed of an OPA145IDBVR op-amp and 100 MΩ feedback resistor for a gain of 10^8 V/A. Power to the op-amp is filtered with capacitors (see Supplmentary Materials [7])

freely available in the supplementary information [7].

II. THEORETICAL BACKGROUND

A. Tunneling probability

We begin by modeling the tip-sample gap as a one-dimensional trapezoidal potential barrier, where the tunneling probability for an electron of energy E is exponential with barrier width Δz,

$$|\psi(x)|^2 \propto e^{-2\sqrt{\frac{2m(U-E)}{\hbar}}\Delta z} \approx e^{-A\sqrt{\Phi}\Delta z}.$$

In this expression, m is the mass of an electron, Φ is the work function of the material, U is the average height of the potential barrier, and $A = 2\sqrt{\frac{2m}{\hbar}} \approx 1.025\ \mathrm{eV}^{-1/2-1}$. We use the approximation $E \ll U$. Because tunneling current is proprotional to this probability, the exponential dependence can be probed experimentally with I-z.

B. Tunneling spectroscopy

Figure 2 shows a schematic of one-dimensional tunneling, which is used to model tunneling between the tip and sample. The full tunneling current I_{tunnel} is composed not just of electrons having energy E, but of electrons having energy between eV_{bias} and the Fermi level [8]:

$$I = \frac{4\pi e}{\hbar}\int_0^{eV} \rho_{tip}(E-eV)\rho_{sample}(E)T(E,V,d)\,dE,$$

where ρ_{tip} and ρ_{sample} are the electronic densities of states of the tip and sample, respectively, and $T(E,V,d)$ is the transmission probability at energy E, bias V, and barrier width d. As shown in Fig. 2(a), when $V_{bias} < 0$, the energies of electrons in the sample increase, and the tunneling current consists of occupied states in the sample flowing into unoccupied states in the tip. For $V_{bias} < 0$ (Fig. 2(b)), the energies in the sample decrease, and electrons flow from occupied states in the *tip* to unoccupied states in the sample. When $V_{bias} = 0$, there is equal probability that electrons tunnel from tip to sample as vice versa, so no net current flows.

For a metallic tip with constant density of states and no surface contamination (such as Pt:Ir in air):

$$\frac{dI}{dV} \propto \rho_{sample}(eV).$$

C. Categories of electronic structure

In designing instructional materials to support this advanced undergraduate lab, we organize potential test samples into three main types. Qualitative observations of differences in electronic structure between metals, semimetals,

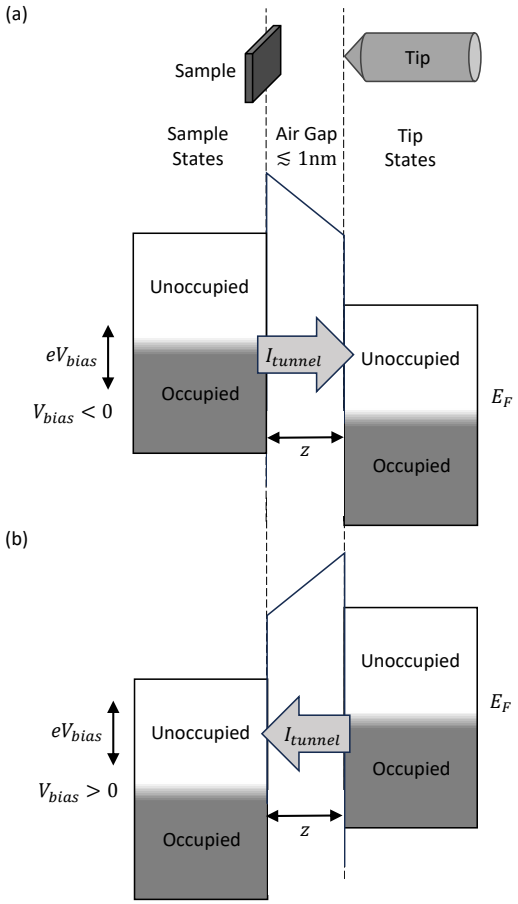

FIG. 2. Schematic energy diagram for the tip-sample junction for differing V_{bias}. (a) $V_{bias} < 0$. Sample states are shifted higher in energy, and current flows from sample to tip. (b) $V_{bias} > 0$. Sample states are shifted lower in energy, and current flows from tip to sample.

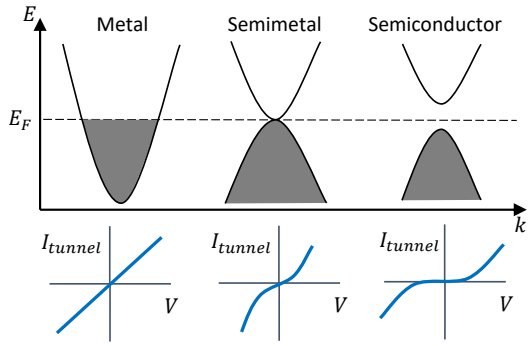

FIG. 3. Simplified schematics of band structure (upper) and sketches of associated tunneling I-V curves (lower) in a metal, semimetal, and semiconductor. In ZTM experiments, applying V_{bias} to the sample probes states above and below the Fermi level E_F for $V_{bias} < 0$ and $V_{bias} > 0$, respectively.

and semiconductors can be made from I-V alone [9]. Figure 3 shows simplified schematics of the band structure in a metal, semimetal, and semiconductor. In a metal, the electronic density of states is roughly constant with energy for small V_{bias} ($\lesssim 1$ V). Thus, the tunneling conductance is also constant, resulting in a linear I-V curve. The semimetal band structure schematic shown in Fig. 3 resembles that of HOPG. For energies near E_F, the available states are limited, resulting in a reduction of tunneling conductance for small values of V_{bias} compared with larger values. The conductance is non-zero for all voltages, giving the 'S'-shaped I-V curve. Finally, a semiconductor has no available states, as the E_F lies within the band gap. Thus, the tunneling conductance is zero for small V_{bias}, and non-zero once V_{bias} is adjusted to probe states in the conduction band or valence band. The I-V curve is zero within the band gap and non-zero for energies above the band gap. Tunneling spectroscopy can measure the width of the band gap in a semiconductor, with energy resolution 3.5 k_BT. At room temperature this is ~ 90 meV, which is an order of magnitude smaller than the band gap in typical semiconductors, such as Si (1.1 eV).

III. TUNNELING MICROSCOPE DESIGN

Figure 4 shows the system schematic of the ZTM with updated, compact control electronics. The physical microscope is constructed out of two Al slabs. The tunneling tip is attached to a piezo transducer (Thorlabs PC4FL) near the fulcrum, giving a mechanical lever advantage. For large adjustments of the stepper motor, the tip moves slowly to bring it within tunneling distance without making contact with the sample. A detailed description and list of materials in the microscope body may be found in Ref. [6].

In this paper we describe work integrating the control electronics into an enclosed control board and pre-amp board. (The previous iteration of the device relied on multiple benchtop power supplies and routing signals through a separate, large breakout box.) We have also made the pc board drawings and design files (for Altium software) available for download (see Supplementary Materials, [7]).

To control the instrument, we use software written in LabVIEW and a DAQ device from National Instruments (NI USB-6259). However, the user can select whichever DAQ and software controller they are comfortable with. The control software written for LabVIEW can be obtained by contacting the corresponding author.

The analog and digital logic signals are routed from the DAQ device to the control board (Fig. 4). The board is placed in a metal enclosure (Digi-Key 377-2313-ND) and powered by plugging into 120 V_{ac} wall power. The supply on the board outputs power to the on-board stepper motor driver (Sparkfun ROB12779), and the op-amp (OPA145IDBVR) in the current-voltage pre-amplifier circuit on a separate board. The analog signals (V_{piezo}, I_{tunnel}, and V_{bias}), stepper driver outputs, and power for the op-amp are then routed through

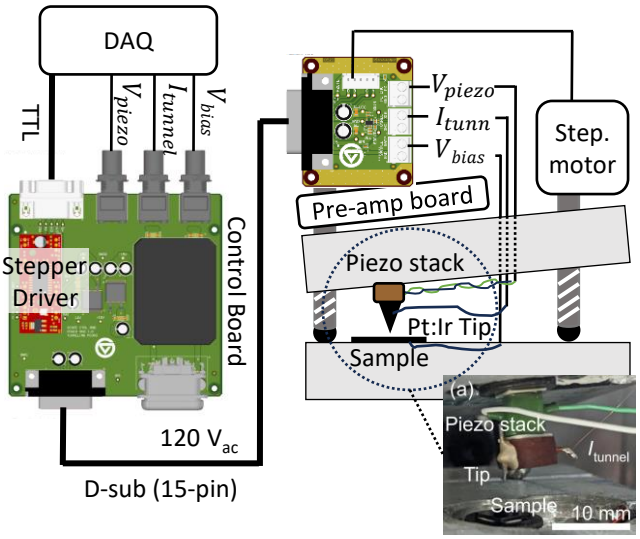

FIG. 4. The updated ZTM design schematic. The main body is composed of two Al slabs that use lever advantage to approach the tip toward the sample sufficiently slow to bring it within tunneling range without crashing. The tip is attached to the piezo stack near the fulcrum, just above the sample. The inset shows a photo of the assembly (marked with (a); Reprinted from R. Lindgren *et al.*, Am. J. Phys. **90**, 795-800 (2022), with the permission of AIP Publishing.). The tip is held in a 23 GA syringe that is silver-epoxied to a length of magnet wire carrying the tunneling current. Analog and digital signals are routed from the DAQ through the control board (labeled). The control board connects to 120 V mains and powers the op-amp on the pre-amp board and the stepper motor driver. All signals are then routed through the 15-pin D-sub cable to the pre-amp board (labeled), containing the current-voltage amplifier. The stepper motor (used for inital approach) also connects to this pre-amp board. The analog signals, V_{piezo}, I_{tunnel}, and V_{bias} are routed through bore holes in the top Al slab where they connect to the scan head and sample.

a cable with 15-pin D-sub connector, to the pre-amp board. The pre-amp board is fixed to the top Al slab. The three analog signals connect to three screw terminals on the opposite side of the pre-amp board. To protect the wires that carry these signals from mechanical damage, they are routed through holes and grooves bored into the Al slabs. Finally, to shield the device from electronic noise, we cover it with a grounded metal enclosure. While we have opted for steel enclosures with feed-throughs for the cable, we have also found that a cardboard box lined with grounded Al foil can shield noise just as well.

IV. RESULTS

We note that experimental results presented in this paper were obtained with the original control electronics described in Ref. [6]. The new integrated control electronics described in Section III have been successfully tested using a 1 GΩ re-

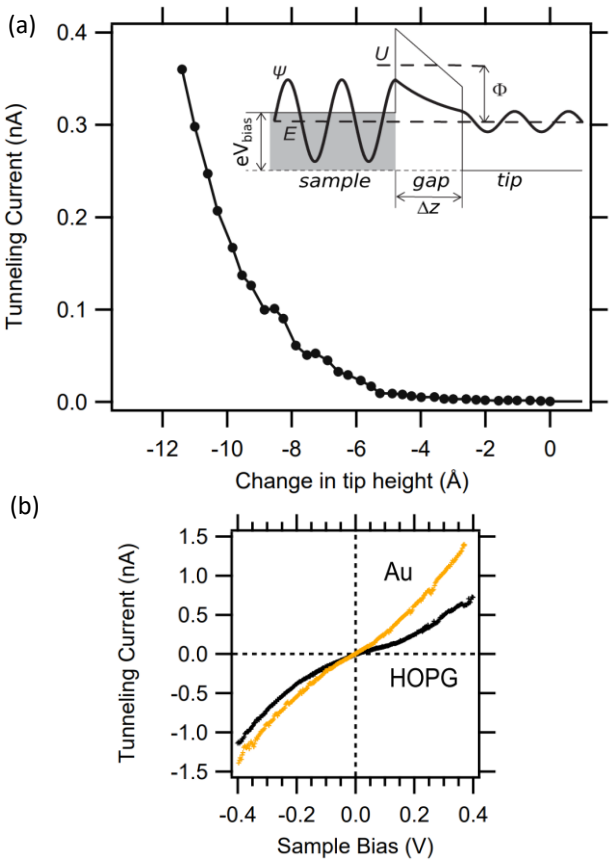

FIG. 5. Representative I-Δz and tunneling spectroscopy data. (a) I-Δz for HOPG sample showing the exponential dependence of the tunneling barrier width (tip-sample gap). The inset shows a schematic energy diagram of the 1D potential model. (b) Tunneling spectroscopy comparison of metal (thin-film Au) and semimetal (HOPG) samples. Data were obtained with original control electronics described in Ref. [6]. Reprinted from R. Lindgren *et al.*, Am. J. Phys. **90**, 795-800 (2022), with the permission of AIP Publishing.

sistor (tunneling conductances of actual tunnel junctions are of order 1-10 GΩ). However, the new electronics could not be tested on the actual ZTM tunnel junction before the submission due date of these Proceedings.

Figure 5(a) shows I-Δz curves obtained from an HOPG sample. Beginning with the tip in range, the current was recorded while pulling the tip back away from the sample allowing the tunneling current to decrease to zero. The objective here is not to make firm contact with the surface, which would damage the tip and affect its ability to obtain stable tunneling current. Thus, it is not possible to know the absolute tip-sample distance, but distances relative to the starting point (Δz) are sufficient. Distances are determined by using manufacturers' calibration curves. Students will analyze these data sets by plotting on a semilog scale and applying a linear fit. Detailed examples of this process were described in Ref. [6].

Figure 5(b) shows a comparison of tunneling spectroscopy curves (I-V) for a metal (Au) and semimetal (HOPG). The metallic Au density of states are approximately constant, thus the constant slope predicted in Fig. 3 is observed. By contrast, the tunneling conductance of the semimetallic HOPG is reduced near the Fermi level ($V_{bias} = 0$) as described in Section II C. The reduced tunneling conductance means the slope is smaller near $V_{bias} = 0$ and increases for more positive and more negative V_{bias} where tunneling conductance again increases.

V. CONCLUSIONS

We have designed an apparatus for advanced labs that gives students experience in experimental condensed matter physics while developing technical and practical lab skills as recommended by AAPT [1]. The ZTM is a simplified tunneling microscope intended to expand access to more institutions for students to engage in tunneling spectroscopy experiments and study electronic density of states in undergraduate labs. Plans for fabricating the control pc boards have been made freely available as supplemental material. This tunneling microscope can in principle integrate with diverse existing DAQ devices in departments' infrastructure.

ACKNOWLEDGMENTS

This work was supported in part by a Teaching Innovation Grant from the Faculty Teaching and Learning Center at Grand Valley State University, and by a grant from the Center for Scholarly and Creative Excellence at Grand Valley State University.

[1] J. Kozminski *et al.*, AAPT Recommendations for the Undergraduate Curriculum (2014).
[2] G. Binnig *et al.*, Appl. Phys. Lett. **40**, 178-180 (1982).
[3] G. Binnig *et al.*, Phys. Rev. Lett. **55**, 9 (1985).
[4] S.I. Park and C. F. Quate, Appl. Phys. Lett. **48**, 112-114 (1986).
[5] R. Sonnenfeld and P. K. Hansma, Science **232**, 211-213 (1986).
[6] R. Lindgren *et al.*, Am. J. Phys. **90**, 795-800 (2022).
[7] (link pending, will be available with BFY proceedings)
[8] J. Bardeen, Phys. Rev. Lett. **6**, 57-59 (1961).
[9] J. A. Stroscio, R. M. Feenstra, and A. P. Fein, Phys. Rev. Lett. **57**, 2579-2582 (1986).